Atmos. Chem. Phys., 11, 2881–2892, 2011
www.atmos-chem-phys.net/11/2881/2011/
doi:10.5194/acp-11-2881-2011

Atmospheric Chemistry and Physics

Distribution and air-sea exchange of mercury (Hg) in the Yellow Sea

Z. J. Ci[1], X. S. Zhang[1], Z. W. Wang[1], Z. C. Niu[1], X. Y. Diao[2], and S. W. Wang[2]

[1]State Key Laboratory of Environmental Chemistry and Ecotoxicology, Research Center for Eco–Environmental Sciences, Chinese Academy of Sciences, Beijing, China
[2]Institute of Oceanology, Chinese Academy of Sciences, Qingdao, China

Received: 17 December 2010 – Published in Atmos. Chem. Phys. Discuss.: 19 January 2011
Revised: 17 March 2011 – Accepted: 21 March 2011 – Published: 28 March 2011

Abstract. The Yellow Sea, surrounded by East China and the Korea Peninsula, is a potentially important receptor for anthropogenic mercury (Hg) emissions from East Asia. However, there is little documentation about the distribution and cycle of Hg in this marine system. During the cruise covering the Yellow Sea in July 2010, gaseous elemental mercury (GEM or Hg(0)) in the atmosphere, total Hg (THg), reactive Hg (RHg) and dissolved gaseous mercury (DGM, largely Hg(0)) in the waters were measured aboard the *R/V Kexue III*. The mean (±SD) concentration of GEM over the entire cruise was $2.61 \pm 0.50\,\mathrm{ng\,m^{-3}}$ (range: 1.68 to $4.34\,\mathrm{ng\,m^{-3}}$), which were generally higher than other open oceans. The spatial distribution of GEM generally reflected a clear gradient with high levels near the coast of East China and low levels in open waters, suggesting the significant atmospheric Hg outflow from East China. The mean concentration of THg in the surface waters was $1.69 \pm 0.35\,\mathrm{ng\,l^{-1}}$ and the RHg accounted for a considerable fraction of THg (RHg: $1.08 \pm 0.28\,\mathrm{ng\,l^{-1}}$, %RHg/THg = 63.9%). The mean concentration of DGM in the surface waters was $63.9 \pm 13.7\,\mathrm{pg\,l^{-1}}$ and always suggested the supersaturation of Hg(0) in the surface waters with respect to Hg(0) in the atmosphere (the degree of saturation: 7.8 ± 2.3 with a range of 3.6–14.0). The mean Hg(0) flux at the air-sea interface was estimated to be $18.3 \pm 11.8\,\mathrm{ng\,m^{-2}\,h^{-1}}$ based on a two-layer exchange model. The high wind speed and DGM levels induced the extremely high Hg(0) emission rates. Measurements at three stations showed no clear vertical patterns of DGM, RHg and THg in the water column. Overall, the elevated Hg levels in the Yellow Sea compared with other open oceans suggested that the human activity has influenced the oceanic Hg cycle downwind of East Asia.

Correspondence to: X. S. Zhang
(zhangxsh@rcees.ac.cn)

1 Introduction

Mercury (Hg) is a persistent pollutant of global concern known to be transported long distances in the atmosphere into remote ecosystems (Schroeder and Munthe, 1998). Hg subsequently transfers to methylmercury (MMHg) and accumulates into the food chain (Morel et al., 1998; USEPA, 1997; Fitzgerald et al., 2007). Consumptions of fish with high MMHg levels can lead to adverse health effects in humans and wildlife (USEPA, 1997). Therefore, there is an increasing interest to understand the global biogeochemistry of mercury.

Numerous studies suggested that the Hg cycle in the ocean is one of the key processes in its global biogeochemical cycle (Mason and Sheu, 2002; Seigneur et al., 2001; Strode et al., 2007, 2010; Selin et al., 2007; Hedgecock et al., 2006; Soerensen et al., 2010b). It has been well-established that the atmospheric Hg deposition is the principal source of Hg to open ocean (Mason and Sheu, 2002; Lindberg et al., 2007). In earlier studies, the wet deposition was considered the only primary pathway (Mason et al., 1994). Recently, due to the significant instrumental improvement for atmospheric Hg speciation measurements (Landis et al., 2002), increasing field studies have shown that gaseous elemental mercury (GEM, or Hg(0)) in the marine boundary layer (MBL) can be rapidly oxidized to form reactive gaseous mercury (RGM) in situ (e.g., Hedgecock et al., 2003; Laurier et al., 2003; Laurier and Mason, 2007; Chand et al., 2008; Sprovieri et al., 2003, 2010a; Soerensen et al., 2010a). Because of the high water solubility and surface reactivity, the dry deposition of RGM (direct or uptake by sea-salt aerosol) represents an important fraction of Hg deposition flux to the ocean (Mason and Sheu, 2002; Holmes et al., 2009).

Divalent Hg (Hg(II)) is the dominant Hg species of the atmospheric deposition to the ocean (Lindberg et al., 2007). Once deposited, Hg(II) in the water can convert to DGM (largely Hg(0)) mediated by the photochemistry (e.g.,

Amyot et al., 1997; Lanzillotta et al., 2002) and the microbe activity (e.g., Rolfhus and Fitzgerald, 2004; Fantozzi et al., 2009), leading to the surface water supersaturation of Hg(0) with respect to the atmospheric Hg(0) (Kim and Fitzgerald, 1986; Amyot et al., 1997; Andersson et al., 2007). Supersaturation of Hg(0) in the surface water implies a net emission of Hg(0) from the sea surface to the atmosphere. The oceanic transformation reaction and subsequent emission to the atmosphere of Hg(0) is a critical fraction of the global Hg cycle (Strode et al., 2010). Mason and Sheu (2002) estimated that the Hg(0) re-emission from the sea surface was approximately equivalent to the global anthropogenic emission source. Using an updated global atmospheric Hg model coupled with a mixed layer slab ocean, Soerensen et al. (2010b) indicated that the Hg(0) re-emission constitutes 80% of the previously atmospheric Hg deposition flux.

The Yellow Sea is located in the downwind region of East Asia, which is the strongest anthropogenic Hg emission source in the world (Pacyna et al., 2010). High anthropogenic Hg emissions with a considerable fraction of RGM and PHg (Schroeder and Munthe, 1998) can induce the elevated atmospheric Hg deposition, probably resulting in a corresponding increase in the oceanic Hg pool. Other pollutions and nutrients input to the Yellow Sea via the river/sewage discharge and atmospheric deposition have influenced the nutrient structure and biogeochemistry of this marine ecosystem (Liu et al., 2003). This change may potentially affect the behavior and fate of Hg in the Yellow Sea. However, there is little documentation of Hg distribution and cycle in this marine environment due to the challenge of ultra-trace Hg analysis. Here, based on the measurements of various Hg species in the MBL and the waters of the Yellow Sea during the cruise in July 2010, we investigated the distribution of Hg (GEM in the atmosphere, total Hg, reactive Hg and DGM in the water) in this marine environment and further estimated the Hg(0) flux at the air-sea interface.

2 Methods

2.1 Site region

The Yellow Sea is a semi-closed marginal sea and a representative shallow continental shelf sea with an average depth of about 40 m. It is the link for material and energy exchange between the Bohai Sea (inner sea) and the East China Sea. The hydrological characteristics of this region are impacted by the Bohai Sea waters, the China and Korea costal waters and the East China Sea open waters. Several rivers heavily impacted by human activities (including Huaihe, Yalu, Han, Taedong and Geum Rivers) carrying large land-sourced materials enter the Yellow Sea. This marine region is an important fishing area in East Asia because the special current field induces the high nutrient concentrations and subsequently results in high primary production.

This open cruise was organized by the Institute of Oceanography Chinese Academy of Sciences (IOCAS) for the duration of 10 days (9–18 July 2010) aboard the *R/V Kexue III*, which circumnavigated the western and central Yellow Sea, originating from Qingdao, through Dalian and Shanghai, and then returned to Qingdao (see Fig. 1).

2.2 Atmospheric GEM measurements

Atmospheric GEM was continually measured using RA-915 + Hg analyzer (Lumex, St. Petersburg, Russia), which based on differential Zeeman Atomic Absorption Spectrometry with High-Frequency Modulation of light polarization (ZAAS–HFM) and a multi-path analytical cell (for more detail on this instrument, see Ci et al., 2011b; Sholupov et al., 2004). This analyzer has been successfully used in various types of GEM measurements (e.g., Southworth et al., 2004; Kim et al., 2006; Wang et al., 2007, Ci et al., 2011a) and showed good agreement with the traditional gold trap/CVAAS system (e.g., WA-4 model, Nippon, Japan, Kim et al., 2006). In this cruise, the analyzer was installed inside the ship laboratory and the ambient air was delivered via a Teflon tube. The air inlet was installed on the upper deck about 8 m a.s.l. to avoid the contamination from ship emissions. Based on three times standard deviation of the system blank, this analyzer has a detection limit of 0.30 ng m^{-3} with sampling time of 1 min at a flow rate of 20 l min^{-1} (Ci et al., 2011b). GEM data with 1-min interval were modified to hourly mean for data analysis. Unfortunately, some air samplings contaminated by the exhaust plume of the *R/V* were found at three occupied stations (GEM concentrations: ∼20–70 ng m^{-3}). Total duration time of the pollution episode was about 2 h and the GEM data in these periods was removed.

2.3 Back-trajectory model

For investigating the influence of air mass movements on the GEM levels, we calculated 72-h back-trajectories of atmospheric transport using the NOAA–HYSPLIT model (Draxler and Rolph, 2003). National Centers for Environmental Prediction's (NCEP) Global Data Assimilation System (GDAS) meteorological dataset was used as the model input (http://www.emc.ncep.noaa.gov/gmb/gdas/). The start height of back-trajectory was 500 m a.s.l., generally representing the typical height of the planetary boundary layer.

2.4 DGM, THg and RHg measurements in the water

2.4.1 Water sampling

This cruise included a total of 47 stations and surface water samples (∼0.5 m depth) for Hg analysis were collected at 40 surface stations, with additional vertical water samples (50–80 m depth) were obtained at three selected stations of these 40 stations (Fig. 1).

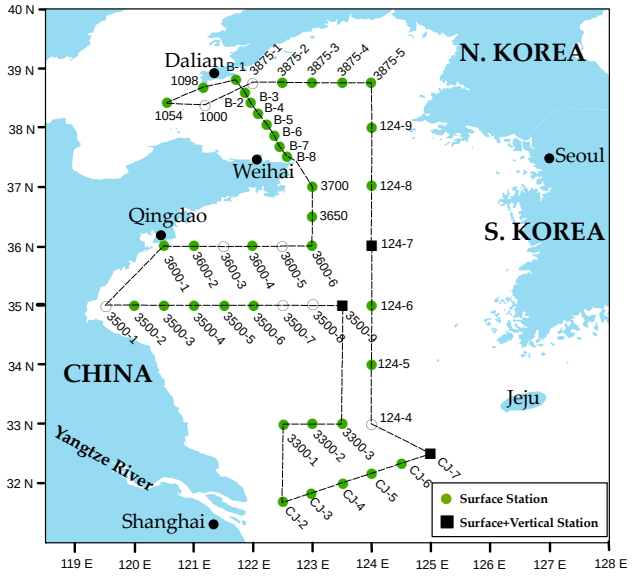

Fig. 1. Cruise track and all stations and stations sampled for Hg in the open cruise 2010 organized by IOCAS along Qingdao–Dalian–Shanghai–Qingdao. Begin day/Station: 9 July 2010/3600–1. End day/Station: 18 July 2010/3500–1.

Ultra-trace Hg clean techniques (USEPA, 2002) were applied during the entire cruise. All containers and Teflon tubes were cleaned in the laboratory by soaking in HNO_3 (20%, v/v) and trace-metal grade HCl (2%, v/v) and rinsed three times with Milli-Q water ($>18.2\,M\Omega\,cm^{-1}$). Powder-free gloves were worn throughout the procedure. The surface water samples were manually collected using a 1 l rigorously acid-washed borosilicate glass bottle. The sampling bottles were rinsed with the water three times prior to collection. There was no headspace within the sampling bottle to avoid loss of DGM by evasion to the headspace. Special attention was paid to the orientation of the *R/V* and wind direction to avoid contamination.

Three stations were selected in the deep region of the Yellow Sea (water depth of 50–80 m) for studying the vertical distribution of Hg. A water sampling system consisting of 12–5 l Teflon lined Go-Flo bottles was used to collect the vertical samples. Samples for Hg analysis were immediately decanted from the Go-Flo bottle into the acid-washed glass bottle.

2.4.2 DGM collection and analysis

A detailed DGM collection and analysis procedure is given by Ci et al. (2011a), following Mason et al. (2001) and Lamborg et al. (2008). Briefly, the water samples were immediately taken to the laboratory aboard the *R/V*, slowly decanted into a 1.5 l borosilicate glass bubbler and purged with the Hg-free ambient air for 30 min at a flow rate of $0.5\,l\,min^{-1}$. The DGM released from water was captured onto the gold trap and sealed with Teflon endcaps and then shipped to the laboratory for analysis. To prevent photolytic reactions, the bubbler covered by the aluminum foil.

The Hg collected in gold trap was quantified using a Cold Vapor Atomic Fluorescence Spectrophotometer (CVAFS, Model III, Brooks Rand, USA) based on the two-stage gold amalgamation method (Gill and Fitzgerald, 1987). The field blanks ($n = 8$) were obtained by replacing the gold trap after the initial purge and the sample was purged for an additional 30 min. The concentrations of DGM in field blanks were $5.0 \pm 2.0\,pg\,l^{-1}$, accounting for 5–10% of the raw DGM in water samples. The method detection limit (three times standard deviations of system blanks) for 1.0 l water sample was $6.0\,pg\,l^{-1}$. All reported DGM concentrations were blank corrected.

After the DGM collections, the subsamples were transferred to the acid-clean bottles, acidified using the trace-metal grade HCl, placed into the double bags and shipped to the laboratory on shore for analysis of total Hg (THg) and reactive Hg (RHg).

2.4.3 THg and RHg determinations

THg and RHg in unfiltered acidified water samples were determined using USEPA Method 1631 for ultra-trace Hg analysis in natural water (USEPA, 2002), following Gill and Fitzgerald (1987) and Balcom et al. (2008). For THg determination, 100 ml samples were pre-oxidized with BrCl, $NH_2OH{\cdot}HCl$ pre-reduction, $SnCl_2$ reduction, Hg-free N_2 purging in a glass bubbler, gold trap pre-concentration, thermal desorption and CVAFS quantification. For RHg determination, 100 ml samples were purged onto the gold trap using Hg-free N_2 after direct reduction with $SnCl_2$ without BrCl pre-oxidation. However, at present the RHg determination in water has not been standardized, as to compare the RHg concentrations obtained by different studies, it is important to take account of the storage and preservation methods adopted by researchers (Parker and Bloom, 2005). Based on the three times standard deviation of the system blank, the detection limits for the THg and RHg were ca. $0.10\,ng\,l^{-1}$.

2.5 Model for estimating air-sea Hg(0) flux

The calculation of air-sea Hg(0) flux and the discussion of its uncertainties are given in Ci et al. (2011a) in detail. Briefly, Hg(0) fluxes were estimated using a two-layer gas exchange model developed by Liss and Slater (1974).

$$F = K_w\,(C_w - C_a/H'), \quad (1)$$

where F is the Hg(0) flux ($ng\,m^{-2}\,h^{-1}$) and K_w is the water mass transfer coefficient ($m\,h^{-1}$). K_w is used as the overall mass transfer coefficient because the resistance to Hg(0) exchange at the air-water interface mainly lies in the water film (> 99%, Poissant et al., 2000). C_w and C_a are Hg(0) concentrations in the surface water (DGM, $pg\,l^{-1}$) and in the

atmosphere (GEM, ng m^{-3}), respectively. H' is the dimensionless Henry's Law constant corrected for the given water temperature.

The gas transfer parameterization of Wanninkhof (1992) was used to calculate the mass transfer coefficient. This parameterization (Eq. 2) has been extensively used to calculate the air–sea Hg(0) fluxes (e.g., Wängberg et al., 2001; Rolfhus and Fitzgerald, 2001; Conaway et al., 2003).

$$K_w = 0.31 u_{10}^2 \, (Sc_{Hg}/660)^{-0.5}, \quad (2)$$

where u_{10} is the wind speed (m s^{-1}) 10 m above the sea surface, Sc_{Hg} is the Schmidt number and defined as,

$$Sc_{Hg} = v/D, \quad (3)$$

where v is the kinematic viscosity (cm^2 s^{-1}) of sea water and D is the aqueous diffusion coefficient (cm^2 s^{-1}) of Hg(0). The kinematic viscosity of sea water at the given temperature is calculated according to the method described by Wanninkhof (1992). The diffusion coefficient of Hg(0) is calculated using the method recently developed by Kuss et al. (2009).

The dimensionless Henry's Law constant is corrected for the desired temperature according to the study of Sanemasa (1975),

$$H' = \frac{M_w 10^{-1078/T+6.250}}{R\rho_w T}, \quad (4)$$

where M_w is the molar weight of water, 18.01×10^{-3} (kg mol^{-1}), R is the gas constant, 8.2058×10^{-2}(atm L K^{-1} mol^{-1}), ρ_w is the density of water, and T is the water temperature (K).

The degree of saturation (S_a) of Hg(0) in the water (DGM) with respect to the atmospheric Hg(0) (GEM) was calculated with Eq. (5).

$$S_a = C_w H'/C_a, \quad (5)$$

where C_w, H', and C_a are as identical as described above. S_a value greater than 1 indicates the supersaturation of DGM, otherwise under saturation is indicated.

3 Results and discussion

3.1 GEM distribution in the MBL

GEM concentrations during the cruise ranged from 1.68 to 4.34 ng m^{-3} with a mean value of 2.61 ± 0.50 ng m^{-3} (median: 2.61 ng m^{-3}). During the past three decades, a large number of GEM/TGM [1] measurements over the ocean have been carried out (Sprovieri et al., 2010b and references therein; Soerensen et al., 2010a). The GEM levels in the MBL over the Yellow Sea was higher than those of oceans in the South Hemisphere, such as the South Atlantic ocean (1.00–1.50 ng m^{-3}, Slemr et al., 2003; Temme et al., 2003; Soerensen et al., 2010a), the Antarctic Ocean (1.30–1.50 ng m^{-3}, Soerensen et al., 2010a), the India Ocean (1.00–1.50 ng m^{-3}, Witt et al., 2010; Soerensen et al., 2010a). Compared with these oceans in the North Hemisphere, the GEM concentrations in the Yellow Sea also were higher than those of many other oceans, such as the Mediterranean Sea (1.5–2.0 ng m^{-3}, Sprovieri et al., 2003, 2010a) and the Adriatic Sea (1.6 ± 0.4 ng m^{-3}, Sprovieri and Pirrone, 2008), but were comparable to the Atlantic Ocean (∼1.5–2.5 ng m^{-3}, Temme et al., 2003; Laurier and Mason, 2007; Soerensen et al., 2010a) and the North Pacific Ocean (2.5 ± 0.5 ng m^{-3}, Laurier et al., 2003). Elevated Hg(0) evasion from the sea surface and long-range transport of anthropogenic emissions from industrial regions might explain those elevated atmospheric Hg levels (Soerensen et al., 2010a).

During the past decade, atmospheric Hg cycle in the downwind region of East Asia has received increasing attentions. Many atmospheric Hg measurements based on the various platforms (including ground, shipborne and airborne) have been conducted. Figure 2 shows the atmospheric Hg measurements at the costal, rural or open ocean regions downwind of China. The GEM/TGM levels reported by all these measurements generally reflected the elevated values compared to the North Hemisphere background regions (e.g., 1.5–1.7 ng m^{-3}, Sprovieri et al., 2010b). The GEM concentrations in this cruise were lower than at sites near the Korea Peninsula (e.g., An-Myun and Jeju, Nguyen et al., 2007, 2010) and were close to those in CST (Ci et al., 2011b), ACE–Asia campaign over the Yellow Sea (Friedli, et al., 2004) and the cruise covering the South China Sea (Fu et al., 2010; Xia et al., 2010), and were slightly higher than those in HSO (Jaffe et al., 2005). The measurements of atmospheric Hg speciation at a high-elevation background station in Taiwan Island (Lulin station) reflected the background levels of atmospheric Hg in the North Hemisphere (Slemr et al., 2009) because this site is generally under the influence of free troposphere (Sheu et al., 2010).

As shown in Fig. 3, the GEM concentrations were generally elevated at the coast of China compared to the open ocean. This supports other studies that showed atmospheric Hg emission from anthropogenic sources in East Asia enhances the atmospheric Hg levels in the downwind region (e.g., Fu et al., 2010; Nguyen et al., 2010). This trend

[1] TGM (total gaseous mercury) = GEM + RGM. Under the normal atmospheric condition, GEM is generally taken more than 95–98% among all atmospheric Hg species. Because RGM easily adsorbs by the surface, some previous TGM measurements should be considered as GEM, especially a filter (usually Teflon) was placed at the inlet of the sample line and/or the long and unheated sampling line was applied. In this paper if there was no otherwise indicated, we did not consider the difference between TGM and GEM, which all refer to the original literatures.

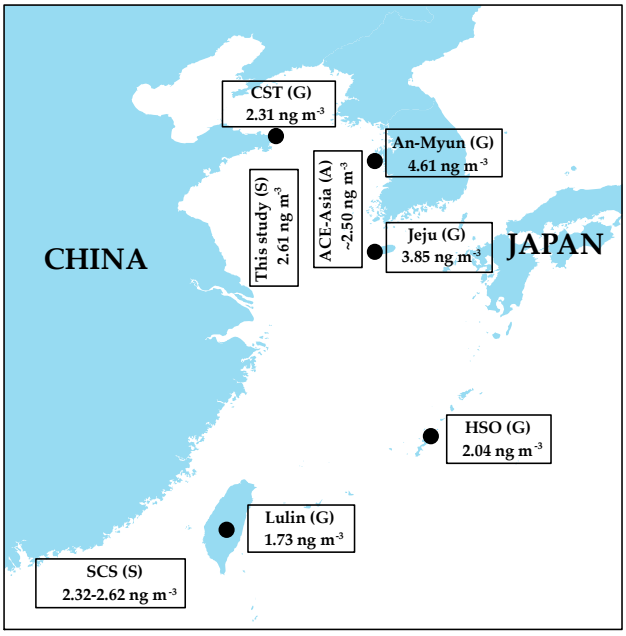

Fig. 2. Comparisons of atmospheric Hg measurements based on various platforms around coastal/open ocean environments of East Asia. (G): ground measurement; (A): airborne measurement and (S): shipborne measurement. CST: Ci et al., (2011b); ACE-Asia: Friedli et al. (2004); An-Myun: Nguyen et al. (2007); Jeju Island: Nguyen et al. (2009); HSO: Jaffe et al. (2005); Lulin: Sheu et al. (2010); SCS: Fu et al. (2010) and Xia et al. (2010).

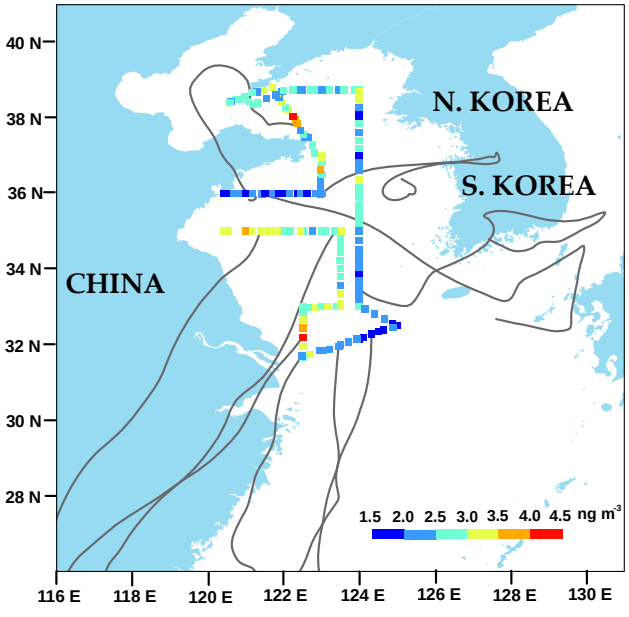

Fig. 3. Atmospheric GEM distribution over the Yellow Sea and the typical back-trajectories of air masses during the cruise in July 2010. See text for more information on the calculation of the back-trajectory.

also has been successfully reproduced by atmospheric modeling (Lin et al., 2010).

The air mass movements also influenced the GEM levels in the study period (see Fig. 3). During 10–11 July 2010 (from Station 3600–1 to 3600–6), although the *R/V* was near the Shandong Peninsula, the GEM levels (2.09 ng m^{-3}) in this period were lower than the campaign average (2.61 ng m^{-3}) and slightly higher than the background levels of the Northern Hemisphere (1.5–1.7 ng m^{-3}, Sprovieri et al., 2010b). The back-trajectories of 500 m showed that the air masses originated from the East China Sea and crossed the Yellow Sea to the *R/V*. The GEM levels in this period were close to those originated from open ocean surface reported by Fu et al. (2010) in the South China Sea cruise. During 12–13 July 2010 (from Station B–8 to 3675–2), the *R/V* navigated along the west coast of the Yellow Sea (near Shandong Peninsula and Liaoning Peninsula). In this period, the GEM concentrations generally fell in 2.50–3.50 ng m^{-3}. The back-trajectory analysis suggested that the air masses in this period largely originated from anthropogenic source regions (such as Shandong Peninsula, Fig. 3). The measurements during 14–17 July (from Station 124–5 to 3500–1) more clearly reflected the influence of air mass movements on the GEM levels. From midday on 14 July to afternoon on 15 July, the air masses originated from the East China Sea before reaching the *R/V* (Fig. 3). The GEM concentrations in this period were very close to those of Stations 3600–1 to 3600–6, reflecting the regional background GEM levels of East Asia. As the *R/V* progressed, the source region of the air masses moved from the East China Sea to the southeastern coast of China. At 00:00 h on 16 July the air masses reaching the *R/V* had passed directly over large industrial and port areas around Southeast China (Fig. 3). The GEM concentrations started to sharply increase from ca. 2.00 ng m^{-3} to 4.00 ng m^{-3} and remained ca. 3.00–3.50 ng m^{-3} in last period of the cruise (from Station 3300–1 to 3500–1).

3.2 THg and RHg in the surface water

The mean concentration of THg in the surface waters was 1.69 ± 0.35 ng l^{-1} with a range of 0.89–2.26 ng l^{-1}, which were higher than those in open ocean, such as the Pacific Ocean (0.23 ng l^{-1}, Laurier et al., 2004), the Mediterranean Sea (0.26–0.30 ng l^{-1}, Horvat et al., 2003; Kotnik et al., 2007), the Atlantic Ocean (~0.5–0.6 ng l^{-1}, Mason et al., 1998; Mason and Sullivan, 1999), the Black Sea (0.32–2.08 ng l^{-1}, Lamborg et al., 2008) and were comparable to values reported in some near-shore environments, such as the Long Island Sound (0.46–3.98 ng l^{-1}, Rolfhus and Fitzgerald, 2001) and the Connecticut River estuary, ~2.0 ng l^{-1}, Rolfhus et al., 2003), and lower than the measurements in the coastal site of the Yellow Sea (2.68 ng l^{-1}, Ci et al., 2011a). In the estimate of the global anthropogenic Hg emissions, Pacyna et al. (2010) suggested that the anthropogenic atmospheric Hg emissions from Asia contribute about half

of the global emission sources. For the anthropogenic Hg emission, RGM and particulate Hg (PHg) generally present a large fraction and they deposit quickly due to the high water solubility and surface reactivity (Schroeder and Munthe, 1998). Because the Yellow Sea is located on the Eastern Asian continental margin and surrounded by the industrial zone of East China and Korea, the atmospheric wet/dry deposition can contribute to the Hg pool of this marine system (Lin et al., 2010). Recently, Fu et al. (2010) reported the THg levels of 1.2 ng l^{-1} in the South China Sea, which were slightly lower than our study and also were higher than those of open oceans.

The spatial distribution of THg in the surface waters is illustrated in Fig. 5. The mean THg concentration of water samples taken from stations within 100 km from land ($n = 22$) was significantly higher than those of other stations (t-test, $p < 0.001$), suggesting the terrestrial source and resuspended sediment might slightly enhance the THg concentration in the near-shore water column. Stations CJ–2 to CJ–7 are near the Yangtze River mouth and under the influence of Yangtze Diluted Water (low salinity in surface water of Station CJ–7, see Fig. 6); however, the mean concentration of THg for these six stations was no significantly higher than those of other stations (t-test, $p = 0.662$). The studies of Hg accumulation in the estuary of the Yangtze River suggested that the estuary is an important sink for aquatic Hg (Shi et al., 2005; Fang and Chen, 2010). Based on the estimate of Fang and Chen (2010), about 50% of the Hg from river discharge was accumulated in the sediment of the shore. Then the low THg levels of Stations CJ–2 to CJ–7 might be explained by that the six stations were far from the river mouth and the Hg input via river discharge had been removed by the sedimentation process in the coastal region because of the high coefficient between aquatic Hg and suspend particulate matter (Fitzgerald et al., 2007). However, more detailed integrated researches on the Hg cycle in river-delta-estuary-sea ecosystems of the Yangtze River are urgently needed.

The mean RHg concentration in the cruise was 1.08 ± 0.28 ng l^{-1} with a range of 0.54–1.66 ng l^{-1}, which accounted for the dominant fraction of THg (%RHg/THg = 63.9%). The RHg concentrations in the Yellow Sea were generally higher than many other open oceans (e.g., Atlantic Ocean: 0.34 ng l^{-1}, Mason and Sullivan, 1999; Mediterranean Sea: 0.09 ng l^{-1}, Horvat et al., 2003) and were higher or comparable to those of near-shore environments (e.g., Long Island Sound: 0.26–0.90 ng l^{-1}, Rolfhus and Fitzgerald, 2001; Lower St. Lawrence Estuary: <0.04–0.22 ng l^{-1}, Cossa and Gobeil, 2000). However, the RHg/THg ratios of 63.9% in the Yellow Sea were higher than many other near-shore environments (e.g., 20% in Long Island Sound and Lower St. Lawrence Estuary, Rolfhus and Fitzgerald, 2001; Cossa and Gobeil, 2000) and were similar to those in open oceans (e.g., 60% in the Atlantic Ocean, Mason and Sullivan, 1999; 57% in the Mediterranean Sea, Horvat et al., 2003). Because the

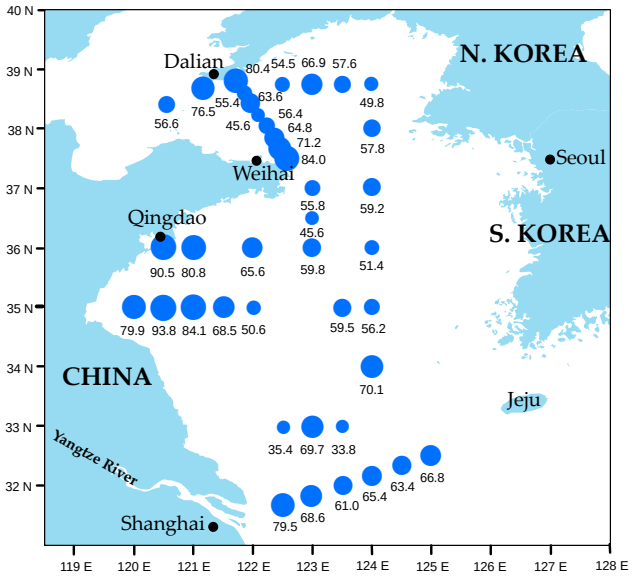

Fig. 4. Spatial distribution of DGM (unit in pg l^{-1}) in the surface waters of the Yellow Sea during the cruise in July 2010.

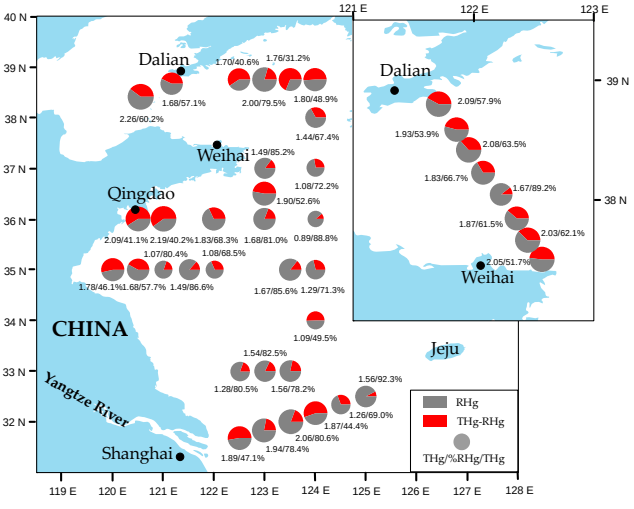

Fig. 5. Spatial distribution of the total Hg (THg, unit in ng l^{-1}) and reactive Hg (RHg) and RHg/THg ratios in the surface waters of the Yellow Sea during the cruise in July 2010.

RHg in aquatic ecosystem is generally considered as the fraction of Hg for the biogeochemical transformation (e.g., reduction to Hg(0) and methylation to MMHg, Morel et al., 1998 and references therein; Amyot et al., 1997; Whalin et al., 2007), the high RHg levels and RHg/THg ratios suggest that the turnover time of Hg in the Yellow Sea may be shorter than other marine systems and potentially indicate the more dynamic cycling of Hg in this marine system.

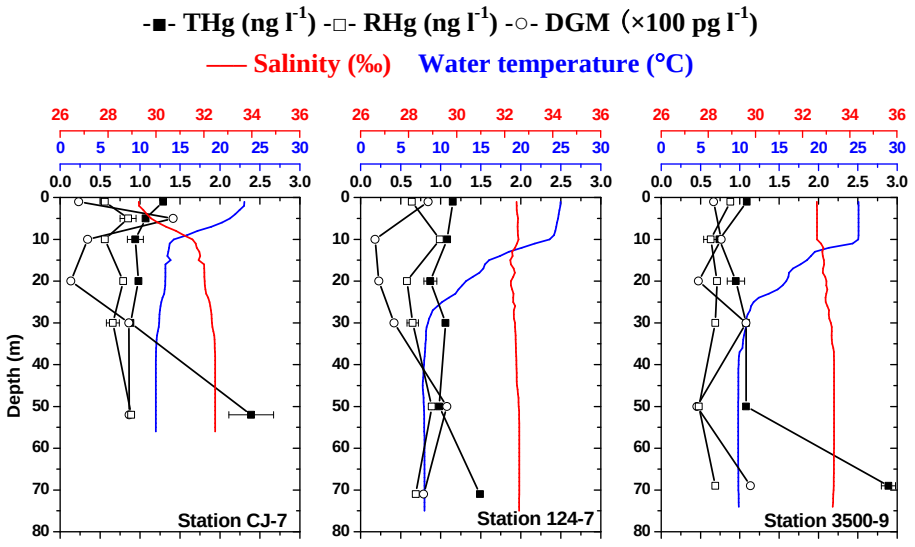

Fig. 6. Vertical distribution of total Hg (THg), reactive Hg (RHg), dissolved gaseous mercury (DGM, largely Hg(0)), water temperature and salinity in the water column at three stations (Station CJ–7: 32.50° N, 124.99° E; Station 124–7: 36.00° N, 124.00° E and Station 3500–9: 35.00° N, 123.50° E).

3.3 DGM concentrations in the surface water, S_a and air-sea Hg(0) flux

3.3.1 DGM concentrations

The DGM concentrations in the surface waters ranged from 33.8 pg l^{-1} to 93.8 pg l^{-1} with the mean concentration of 63.9 ± 13.7 pg l^{-1}, which accounted for 3.6% of the Hg pool of water (%DGM/(THg + DGM)). The ratios were generally comparable to those in near-shore environments (e.g., Rolfhus et al., 2001; Ci et al., 2011a) and were lower than those in open oceans (e.g., Mason et al., 1998; Kotnik et al., 2007). The DGM concentrations in the Yellow Sea were generally higher than those observed from most of open oceans, such as the Equatorial Pacific Ocean (6–45 pg l^{-1}, Kim and Fitzgerald, 1986), the Mediterranean Sea (30–46 pg l^{-1}, Horvat et al., 2003; Kotnik et al., 2007), the Arctic Ocean (44 pg l^{-1}, Andersson et al., 2008b), the Baltic Sea (17.6 pg l^{-1}, Wängberg et al., 2001) and were comparable to those observed from some open oceans, such as the North Sea (20–160 pg l^{-1}, Baeyens and Leermakers, 1998), and costal regions, such as the Tokyo Bay (52 pg l^{-1}, Narukawa et al., 2006), the Swedish coast (40–100 pg l^{-1}, Gårdfeldt et al., 2001) and the Scheldt Estuary (40–108 pg l^{-1}, Baeyens and Leermakers, 1998). During the summer of 2007, Fu et al. (2010) reported that the mean DGM concentration of 36.5 pg l^{-1} in the South China Sea, which also were lower than the Yellow Sea. Recently, for understanding the seasonal and diurnal variations of DGM in the coastal region of the Yellow Sea, we conducted the DGM measurements covered four seasons at CST (site location refers to Fig. 2) during 2008–09 (Ci et al., 2011a). This measurement showed a seasonal variation of DGM with elevated levels in warm seasons and low levels in cold seasons. Interestingly, the measurement in the summer campaign (August 2009) at CST suggested the highest seasonal average with 69.0 pg l^{-1} (Ci et al., 2011a), which was consistent with this cruise. Figure 4 illustrates the spatial distribution of DGM and generally showed the significantly high levels in near coast stations (within 100 km) and low levels in open waters (t-test, $p < 0.001$). This trend has been extensively reported (e.g., Fu et al., 2010).

As mentioned in the Introduction, many field measurements and laboratory incubation experiments indicated that the DGM formation in the water column is mediated by the abiotic and biotic mechanisms. Among all factors, the solar radiation (Amyot et al., 1997; Lanzillotta et al., 2002; Rolfhus and Fitzgerald, 2004) and microorganism activities (Mason et al., 1995; Lanzillotta et al., 2004; Poulain et al., 2004; Fantozzi, et al., 2009) are considered as the principal forces for the RHg reduction to DGM. The high DGM levels in this cruise and elevated levels near coast might be explained as follows. First, this cruise was conducted in July, corresponding to the high solar radiation, which would promote the photochemical reduction of RHg. Second, due to the special current pattern, the river input and the atmospheric deposition of nutrients (e.g., N and P), the primary production in the Yellow Sea is high (Liu et al., 2003), then the RHg reduction mediated by biochemical processes may be promoted and subsequently contributes to the elevated DGM levels. Particularly, in recent years the massive green algae (*Enteromorpha prolifera*) blooming often occurred in the coastal region of the Yellow Sea in the period of post spring to early summer (Sun et al., 2008). In this cruise, we

also observed the green algae bloom, which might directly or indirectly stimulate the DGM formation via organism activity in the water column, especially the coastal region. Interestingly, we did not find strong correlation between DGM and THg/RHg in this study, which was consistent with our previous study at the coastal site (CST) of the Yellow Sea (Ci et al., 2011a). This result might further indicate the importance of biochemical processes on the DGM formation in the Yellow Sea. However, at present, there is no focused study is performed to investigate the influence of green algae blooming on the Hg cycle in this marine environment.

3.3.2 Degree of DGM saturation

The mean degree of DGM saturation (S_a) was 7.8 ± 2.3 with a range of 3.6–14.0, indicating that there was always supersaturation of Hg(0) in the surface waters with respect to Hg(0) in the atmosphere (Table 1). This S_a values were higher than some marine environments (e.g., 3.51 ± 2.67 in the Long Island Sound, Rolfhus and Fitzgerald, 2001) and were comparable to those measurements in coastal site (CST) of the Yellow Sea in summer 2009 (Ci et al., 2011a) and the South China Sea in July 2007 (Fu et al., 2010). Comparable values also were reported in some studies performed in warm seasons, such as 4–40 in the Pacific Ocean (Mason and Fitzgerald, 1993), ∼7–8 in the Mediterranean Sea (Andersson et al., 2008b; Gårdfeldt et al., 2003) and 10 in the Tokyo Bay (Narukawa et al., 2006), although special attention should be paid to that some studies mentioned above (Fu et al., 2010; Andersson et al., 2008b) used a different Henry's law constant developed by Andersson et al. (2008a).

3.3.3 Air-sea Hg(0) flux

The supersaturation of Hg(0) in the surface waters indicated that the exchange of Hg(0) would be always from the sea surface to the atmosphere. The mean Hg(0) flux at the air-sea interface in the entire cruise was $18.3 \pm 11.8\,\mathrm{ng\,m^{-2}\,h^{-1}}$. The maximum with $44.0\,\mathrm{ng\,m^{-2}\,h^{-1}}$ was estimated at Station 3600–2 (at 17:46 LT on 10 July 2010, UTC+08:00) and the minimum with $3.2\,\mathrm{ng\,m^{-2}\,h^{-1}}$ at Station 124–8 (at 05:12 LT on 14 July 2010, UTC+08:00) (Table 1). These fluxes were 5–10 times higher than most of marine environments, such as the Pacific Ocean (∼$3\,\mathrm{ng\,m^{-2}\,h^{-1}}$, Kim and Fitzgerald, 1986; Mason and Fitzgerald, 1993), the Mediterranean Sea (1.52–$4.92\,\mathrm{ng\,m^{-2}\,h^{-1}}$, Andersson et al., 2007; 4.2–$7.9\,\mathrm{ng\,m^{-2}\,h^{-1}}$, Gårdfeldt et al., 2003); the Arctic Ocean ($2.4\,\mathrm{ng\,m^{-2}\,h^{-1}}$, Andersson et al., 2008b), and also were higher than those marine environments with similar DGM levels, such as the North Sea (∼2–$6\,\mathrm{ng\,m^{-2}\,h^{-1}}$, Baeyens and Leermakers, 1998), the Tokyo Bay ($5.8 \pm 5.0\,\mathrm{ng\,m^{-2}\,h^{-1}}$, Narukawa et al., 2006) and the Scheldt Estuary (∼6–$12\,\mathrm{ng\,m^{-2}\,h^{-1}}$, Baeyens and Leermakers, 1998). The comparable Hg(0) fluxes were estimated in the Atlantic Ocean (20–$80\,\mathrm{ng\,m^{-2}\,h^{-1}}$) because of the extremely high DGM levels (130–$240\,\mathrm{pg\,l^{-1}}$, Mason et al., 1998; Lamborg et al., 1999). Based on the measurements in summer cruise around the South China Sea, Fu et al. (2010) estimated that the Hg(0) fluxes were 4.5–$3.4\,\mathrm{ng\,m^{-2}\,h^{-1}}$, which were lower than this study.

However, as one evaluates the different works on estimating the air-water Hg(0) flux, it is important to keep in mind that the estimated Hg(0) flux using the two-layer gas exchange model is influenced by the choice of gas transfer parameterizations and diffusion coefficient of Hg(0) (Rolfhus and Fitzgerald, 2001; Andersson et al., 2007; Ci et al., 2011a). According to Eqs. (2) and (3), the relationships between gas transfer velocity and wind speed at 10 m height and the method for estimating D jointly decide the method for calculating K. For a given method for estimating D, the difference between algorithms of K is principally due to adopting the parameter to treat the wind speed. As shown in Fig. 9 in the study of Andersson et al. (2007), five algorithms that widely used for calculating the wind-induced K were compared and suggested that at high wind speed (e.g., $>10\ \mathrm{m\,s^{-1}}$), there was great difference between these algorithms. The parameterization of Wanninkhof (1992) employed in this study represents a moderate strength for calculating K among these five algorithms. The choice of D also influences the calculation of air–sea Hg(0) flux. For example, Kuss et al. (2009) suggested a lower oceanic Hg(0) emission flux using the D developed by Kuss et al. (2009) than Poissont et al. (2000) in a global Hg model (GEOS–Chem, Strode et al., 2007).

As descried in Eq. (1), the Hg(0) flux is jointly determined by the Hg(0) gradient at the air-sea interface and wind-induced K. Because the model is very sensitive to the wind speed, the wind field can temporally influence the Hg(0) exchange (Wanninkhof, 1992; Ci et al., 2011a). According to Eq. (2), the K of wind speed of $15\ \mathrm{m\,s^{-1}}$ (∼$1.0\,\mathrm{m\,h^{-1}}$) and $10\ \mathrm{m\,s^{-1}}$ (∼ $0.4\,\mathrm{m\,h^{-1}}$) is about 10-fold and 4-fold of wind speed of $5\ \mathrm{m\,s^{-1}}$ ($0.1\,\mathrm{m\,h^{-1}}$), respectively. Due to the influence of the Asian Summer Monsoon in this cruise, extremely high wind speed was recorded (see Table 1). This high wind speed principally contributed the elevated Hg(0) emission rates in this cruise.

3.4 Vertical distribution of DGM, RHg and THg in the water column

The vertical samplings at the three selected stations were performed to determine the penetration of these surface signals into the thermocline waters of the Yellow Sea. The data in vertical profiles of THg, RHg, DGM, water temperature and salinity at the three stations (Stations CJ–7, 124–7 and 3500–9) are shown in Fig. 6. On the whole, the distribution of Hg in the three stations showed no clear vertical variations and suggested the comparable levels with the surface stations, indicating the well vertically mixed in the Yellow Sea. The mean THg

Table 1. Summary of station information, atmospheric GEM, surface water DGM and relevant data for air-sea Hg(0) flux calculation in the Yellow Sea during the cruise in July 2010.

Station	Location Lat/Lng	Time yy/mm/dd LT [a]	DGM $pg\,l^{-1}$	GEM $ng\,m^{-3}$	Water temp. °C	Wind speed [b] $m\,s^{-1}$	Saturation %	Flux $ng\,m^{-2}\,h^{-1}$
3600-1	120.50° N/36.00° E	10/07/10 14:50	90.5	1.95	23.0	11.3	14.0	35.0
3600-2	121.00° N/36.00° E	10/07/10 17:46	80.8	2.37	23.0	13.6	10.3	44.0
3600-4	121.99° N/3600° E	10/07/10 23:36	65.6	1.90	25.0	14.1	10.9	40.5
3600-6	122.99° N/3600° E	10/07/11 07:05	59.8	2.20	25.0	11.5	8.6	23.9
3650	122.99° N/36.50° E	10/07/11 10:44	45.6	2.29	25.0	16.4	6.3	35.3
3700	123.00° N/37.00° E	10/07/11 14:39	55.8	3.34	25.0	14.2	5.3	31.2
B-8	122.57° N/37.51° E	10/07/12 06:14	84.0	2.13	24.0	9.4	12.2	22.8
B-7	122.45° N/37.67° E	10/07/12 07:40	71.2	3.00	23.0	6.5	7.2	8.4
B-6	122.36° N/37.85° E	10/07/12 08:49	64.8	2.33	23.0	8.2	8.4	12.5
B-5	122.23° N/38.05° E	10/07/12 10:35	56.4	3.65	23.1	9.0	4.7	11.7
B-4	122.08° N/38.23° E	10/07/12 12:10	45.6	3.27	23.2	9.8	4.2	11.0
B-3	121.96° N/38.42° E	10/07/12 13:43	63.6	2.75	23.3	9.1	7.0	14.8
B-2	121.86° N/38.59° E	10/07/12 15:13	55.4	2.31	24.4	8.6	7.5	12.0
B-1	121.71° N/38.80° E	10/07/12 16:48	80.4	3.18	24.5	8.1	7.9	15.6
1098	121.16° N/38.67° E	10/07/12 19:42	76.5	2.49	24.1	7.0	9.5	11.2
1054	120.55° N/38.41° E	10/07/12 23:19	56.6	2.44	24.0	13.5	7.2	29.7
3875-2	122.49° N/38.75° E	10/07/13 10:15	54.5	2.48	24.3	10.4	6.8	16.9
3875-3	122.99° N/38.75° E	10/07/13 13:31	66.9	2.59	24.1	11.3	8.0	25.0
3875-4	123.50° N/38.75° E	10/07/13 16:08	57.6	2.24	24.8	7.2	8.1	8.9
3875-5	123.99° N/38.75° E	10/07/13 18:54	49.8	2.76	24.6	5.1	5.7	3.6
124-9	124.00° N/38.00° E	10/07/13 23:28	57.8	1.83	24.3	6.3	9.8	6.9
124-8	124.00° N/37.01° E	10/07/14 05:12	59.2	3.01	24.4	4.4	6.1	3.2
124-7	124.00° N/36.00° E	10/07/14 10:59	51.4	2.77	24.8	5.4	5.8	4.2
124-6	124.00° N/35.00° E	10/07/14 16:40	56.2	2.78	25.0	4.6	6.4	3.4
124-5	124.00° N/34.00° E	10/07/14 22:41	70.1	2.11	25.0	4.8	10.5	5.0
CJ-7	124.99° N/32.50° E	10/07/15 09:57	66.8	1.94	25.0	6.5	10.9	8.8
CJ-6	124.50° N/32.34° E	10/07/15 12:35	63.4	1.92	24.0	7.5	10.2	10.8
CJ-5	124.00° N/32.17° E	10/07/15 15:50	64.5	1.78	23.3	7.8	11.0	11.7
CJ-4	123.51° N/32.00° E	10/07/15 19:07	61.0	2.30	23.0	12.2	8.0	25.9
CJ-3	122.98° N/31.83° E	10/07/15 22:11	68.6	2.27	22.0	13.6	8.9	35.9
CJ-2	122.50° N/31.68° E	10/07/16 00:59	79.5	3.34	24.0	12.9	7.4	38.2
3300-1	122.51° N/32.99° E	10/07/16 07:45	35.4	2.26	22.0	12.5	4.6	13.8
3300-2	123.00° N/33.00° E	10/07/16 10:43	69.7	3.36	22.0	13.8	6.1	35.4
3300-3	123.50° N/33.00° E	10/07/16 13:49	33.8	2.85	23.0	15.1	3.6	18.1
3500-9	123.50° N/35.00° E	10/07/16 23:45	59.5	2.92	25.0	12.0	6.4	24.8
3500-6	122.01° N/35.00° E	10/07/17 10:01	50.6	2.97	25.0	11.1	5.4	17.4
3500-5	121.51° N/35.00° E	10/07/17 12:51	68.5	3.05	25.0	5.8	7.1	6.8
3500-4	121.00° N/35.00° E	10/07/17 15:49	84.1	3.28	25.0	4.8	8.1	5.8
3500-3	120.50° N/35.00° E	10/07/17 18:15	93.8	3.18	24.6	7.2	9.2	14.7
3500-2	120.00° N/35.00° E	10/07/17 20:23	79.9	3.29	24.6	11.0	7.6	28.5

[a] Local time, UTC+08:00

[b] Wind speed at 10 m

concentration was $1.26 \pm 0.57\,ng\,l^{-1}$ (0.88–2.39 $ng\,l^{-1}$), $1.10 \pm 0.21\,ng\,l^{-1}$ (0.87–1.49 $ng\,l^{-1}$) and $1.30 \pm 0.79\,ng\,l^{-1}$ (0.74–2.89 $ng\,l^{-1}$) for Stations CJ–7, 124–7 and 3500–9, respectively. The mean %RHg/THg ratio in three stations ranged from 46.0% to 57.1%, indicating the similar value with the surface stations. The elevated THg levels were found at the water–sediment interface (52 m in Station CJ–7 and 69 m in Station 3500–9), probably resulting from the elevated suspend particulate matter due to the resuspension of bottom sediment (Guo et al., 2010).

Compared to the RHg and THg, the vertical distribution of DGM was more variable, further suggesting the dynamic properties of DGM. The DGM levels in the three stations were similar and also comparable to the surface stations, i.e., 13.5–141.4 $pg\,l^{-1}$ ($64.2 \pm 49.1\,pg\,l^{-1}$), 18.0–107.8 $pg\,l^{-1}$ ($59.7 \pm 35.7\,pg\,l^{-1}$) and 45.4–113.6 $pg\,l^{-1}$ ($76.2 \pm 29.2\,pg\,l^{-1}$) for Stations CJ–7, 124–7 and 3500–9, respectively.

4 Conclusions

During the cruise aboard the *R/V Kexue III* from 9–18 July 2010, GEM in the atmosphere, THg, RHg and DGM in the open waters of the Yellow Sea were measured for the first time. The spatial distribution of GEM in the atmosphere, THg and RHg in the water suggested the importance of Hg outflow from East China, which has affected the Hg cycling in the downwind region. The elevated RHg levels and RHg/THg ratios in the waters might indicate the Hg cycle in the Yellow Sea is more active. Using a two-layer gas exchange model, the estimated Hg(0) flux at the interface between atmosphere and the Yellow Sea showed a considerably high levels due to the elevated DGM concentrations and high wind speed.

Acknowledgements. We wish to thank the Open Cruise of Chinese Offshore Oceanography Research organized by the Institute of Oceanology Chinese Academy of Sciences (IOCAS). We thank the personnel from the IOCAS, especially Fei Yu (the chief scientist), Yongshan Zhang (the team captain), Peizhou Cheng (the coordinator) and those involved in the water sampling, for their efforts before, after and during the cruise. We also thank anonymous and named reviewers for their valuable comments and suggestions. This research was funded by the National Natural Science Foundation of China (No. 40803033 and 41073092) and the KIST–CAS project.

Edited by: R. Ebinghaus

References

Amyot, M., Gill, G. A. and Morels, F. M. M.: Production and loss of dissolved gaseous mercury in coastal seawater, Environ. Sci. Technol., 31, 3606–3611, 1997.

Andersson, M. E., Gårdfeldt, K., Wängberg, I., Sprovieri, F., Pirrone, N., and Lindqvist, O.: Seasonal and daily variation of mercury evasion at coastal and off shore sites from the Mediterranean Sea, Mar. Chem., 104, 214–226, 2007.

Andersson, M. E., Gårdfeldt, K., Wängberg, I., and Strömberg D.: Determination of Henry's law constant for elemental mercury, Chemosphere, 73, 587–592, 2008a.

Andersson, M. E., Sommar, J., Gårdfeldt, K., and Lindqvist, O.: Enhanced concentrations of dissolved gaseous mercury in the surface waters of the Arctic Ocean, Mar. Chem., 110, 190–194, 2008b.

Baeyens, W. and Leermakers, M.: Elemental mercury concentrations and formation rates in the Scheldt estuary and the North Sea, Mar. Chem., 60, 257–266, 1998.

Balcom, P. H., Hammerschmidt, C. R., Fitzgerald, W. F., Lamborg, C. H., and O'Connor, J. S.: Seasonal distributions and cycling of mercury and methylmercury in the waters of New York/New Jersey Harbor Estuary, Mar. Chem., 109, 1–17, 2008.

Chand, D., Jaffe, D., Prestbo, E., Swartzendruber, P. C., Hafner, W., Weiss-Penzias, P., Kato, S., Takami, A., Hatakeyama, S. and Kajii, Y.: Reactive and particulate mercury in the Asian marine boundary layer, Atmos. Environ., 42, 7988–7996, 2008.

Ci, Z., Zhang, X., and Wang, Z.: Elemental mercury in coastal seawater of Yellow Sea, China: Temporal variation and air-sea exchange, Atmos. Environ., 45, 183–190, 2011a.

Ci, Z., Zhang, X., Wang, Z., and Niu, Z.: Atmospheric gaseous elemental mercury (GEM) over a coastal/rural site downwind of East China: temporal variation and long-range transport, Atmos. Environ., doi:10.1016/j.atmosenv.2011.02.043, 2011b.

Conaway, C. H., Squire, S., Mason, R. P., and Flegal, A. R.: Mercury speciation in the San Francisco Bay estuary, Mar. Chem., 80, 199–225, 2003.

Cossa, D. and Gobeil, C.: Mercury speciation in the lower St. Lawrence Estuary, Can. J. Fish. Aquat. Sci., 57, 138–147, 2000.

Draxler, R. R. and Rolph, G.D.: HYSPLIT Model access via NOAA ARL READY Website (http://www.arl.noaa.gov/ready/hysplit4.html), NOAA Air Resources Laboratory, Silver Spring, MD, 2003.

Fang, T. H. and Chen, R. Y.: Mercury contamination and accumulation in sediments of the East China Sea, J. Environ. Sci., 22, 1164–1170, 2010.

Fantozzi, L., Ferrara, R., Frontini, F. P. and Dini, F.: Dissolved gaseous mercury production in the dark: Evidence for the fundamental role of bacteria in different types of Mediterranean water bodies, Sci. Total Environ., 407, 917–924, 2009.

Fitzgerald, W. F., Lamborg, C. H., and Hammerschmidt, C. R.: Marine biogeochemical cycling of mercury, Chem. Rev., 107, 641–662, 2007.

Friedli, H. R., Radke, L.F., Prescott, R., Li, P., Woo, J. H. and Carmichael, G. R.: Mercury in the atmosphere around Japan, Korea, and China as observed during the 2001 ACE-Asia field campaign: Measurements, distributions, sources, and implications, J. Geophys. Res., 109, D19S25, doi:10.1029/2003JD004244, 2004.

Fu, X., Feng, X., Zhang, G., Xu, W., Li, X., Yao, H., Liang, P., Li, J., Sommar, J., Yin, R., and Liu, N.: Mercury in the marine boundary layer and seawater of the South China Sea: Concentrations, sea/air flux, and implication for land outflow, J. Geophys. Res., 115, D06303, doi:10.1029/2009JD012958, 2010.

Gårdfeldt, K., Feng, X., Sommar, J., and Lindqvist, O.: Total gaseous mercury exchange between air and water at river and sea surfaces in Swedish coastal regions, Atmos. Environ., 35, 3027–3038, 2001.

Gårdfeldt, K., Sommar, J., Ferrara, R., Ceccarini, C., Lanzillotta, E., Munthe, J., Wängberg, I., Lindqvist, O., Pirrone, N., Sprovieri, F., Pesenti, E., and Strömberg, D.: Evasion of mercury from coastal and open waters of the Atlantic Ocean and the Mediterranean Sea, Atmos. Environ., 37, 73–84, 2003.

Gill, G. A. and Fitzgerald, W. F.: Picomolar mercury measurements in seawater and other materials using stannous chloride reduction and two-stage gold amalgamation with gas phase detection, Mar. Chem., 20, 227–243, 1987.

Guo, X., Zhang, Y., Zhang, F., and Cao, Q.: Characteristics and flux of settling particulate matter in neritic waters: The southern Yellow Sea and the East China Sea, Deep Sea Res., 57, 1058–1063, 2010.

Hedgecock, I. M., Pirrone, N., Sprovieri, F., and Pesenti, E.: Reactive gaseous mercury in the marine boundary layer: modelling and experimental evidence of its formation in the Mediterranean region, Atmos. Environ., 37, 41–49, 2003.

Hedgecock, I. M., Pirrone, N., Trunfio, G. A., and Sprovieri,

F.: Integrated mercury cycling, transport, and air-water exchange (MECAWEx) model, J. Geophys. Res., 111, D20302, doi:10.1029/2006JD007117, 2006.

Holmes, C. D., Jacob, D. J., Mason, R. P., and Jaffe, D. A.: Sources and deposition of reactive gaseous mercury in the marine atmosphere, Atmos. Environ., 43, 2278–2285, 2009.

Horvat, M., Kotnik, J., Logar, M., Fajon, V., Zvonari, T. and Pirrone, N.: Speciation of mercury in surface and deep-sea waters in the Mediterranean Sea, Atmos. Environ., 37, 93–108, 2003.

Jaffe, D., Prestbo, E., Swartzendruber, P., Weiss-Penzias, P., Kato, S., Takami, A., Hatakeyama, S., and Kajii, Y.: Export of atmospheric mercury from Asia, Atmos. Environ., 39, 3029–3038, 2005.

Kim, J. P. and Fitzgerald, W. F.: Sea-air partitioning of mercury in the Equatorial Pacific Ocean, Science, 231, 1131–1133, 1986.

Kim, K. H., Mishra, V. K., and Hong, S.: The rapid and continuous monitoring of gaseous elemental mercury (GEM) behavior in ambient air, Atmos. Environ., 40, 3281–3293, 2006.

Kotnik, J., Horvat, M., Tessier, E., Ogrinc, N., Monperrus, M., Amouroux, D., Fajon, V., Gibicar, D., Zizek, S., Sprovieri, F., and Pirrone, N.: Mercury speciation in surface and deep waters of the Mediterranean Sea, Mar. Chem., 107, 13–30, 2007.

Kuss, J., Holzmann, J., and Ludwig, R.: An elemental mercury diffusion coefficient for natural waters determined by molecular dynamics simulation, Environ. Sci. Technol., 43, 3183–3186, 2009.

Lamborg, C. H., Rolfhus, K. R., Fitzgerald, W. F., and Kim, G.: The atmospheric cycling and air-sea exchange of mercury species in the South and equatorial Atlantic Ocean, Deep Sea Res., 46, 957–977, 1999.

Lamborg, C. H., Yigiterhan, O., Fitzgerald, W. F., Balcom, P. H., Hammerschmidt, C. R., and Murray, J.: Vertical distribution of mercury species at two sites in the Western Black Sea, Mar. Chem., 111, 77–89, 2008.

Landis, M. S., Stevens, R. K., Schaedlich, F., and Prestbo, E. M.: Development and characterization of an annular denuder methodology for the measurement of divalent inorganic reactive gaseous mercury in ambient air, Environ. Sci. Technol., 36, 3000–3009, 2002.

Lanzillotta, E., Ceccarini, C., and Ferrara, R.: Photo-induced formation of dissolved gaseous mercury in coastal and offshore seawater of the Mediterranean basin, Sci. Total Environ., 300, 179–187, 2002.

Lanzillotta, E., Ceccarini, C., Ferrara, R., Dini, F., Frontini, F. P., and Banchetti, R.: Importance of the biogenic organic matter in photo-formation of dissolved gaseous mercury in a culture of the marine diatom *Chaetoceros* sp., Sci. Total Environ., 318, 211–221, 2004.

Laurier, F. and Mason, R.: Mercury concentration and speciation in the coastal and open ocean boundary layer, J. Geophys. Res., 112, D06302, doi:10.1029/2006JD007320, 2007.

Laurier, F. J. G., Mason, R. P., Whalin, L., and Kato, S.: Reactive gaseous mercury formation in the North Pacific Ocean's marine boundary layer: A potential role of halogen chemistry, J. Geophys. Res., 108, 4529, doi:10.1029/2003JD003625, 2003.

Laurier, F. J. G., Mason, R. P., Gill, G. A., and Whalin, L.: Mercury distributions in the North Pacific Ocean – 20 years of observations, Mar. Chem., 90, 3–19, 2004.

Lin, C.-J., Pan, L., Streets, D. G., Shetty, S. K., Jang, C., Feng, X., Chu, H.-W. and Ho, T. C.: Estimating mercury emission outflow from East Asia using CMAQ-Hg, Atmos. Chem. Phys., 10, 1853–1864, doi:10.5194/acp-10-1853-2010, 2010.

Lindberg, S., Bullock, R., Ebinghaus, R., and Engstrom, D.: A synthesis of progress and uncertainties in attributing the sources of mercury in deposition, Ambio, 36, 19–32, 2007.

Liu, S. M., Zhang, J., Chen, S. Z., Chen, H. T., Hong, G.H., Wei, H., and Wu, Q. M.: Inventory of nutrient compounds in the Yellow Sea, Cont. Shelf Res., 23, 1161–1174, 2003.

Liss, P. S. and Slater, P. G.: Flux of gases across the air–sea interface, Nature, 247, 181–184, 1974.

Mason, R. P. and Fitzgerald, W. F.: The distribution and biogeochemical cycling of mercury in the Equatorial Pacific Ocean, Deep Sea Res., 40, 1897–1924, 1993.

Mason, R. P. and Sheu, G. R.: Role of the ocean in the global mercury cycle, Global Biogeochem. Cy., 16, 1093, doi:10.1029/2001GB001440, 2002.

Mason, R. P. and Sullivan, K. A.: The distribution and speciation of mercury in the South and equatorial Atlantic, Deep Sea Res., 46, 937–956, 1999.

Mason, R. P., Fitzgerald, W. F., and Morel, F. M. M.: The biogeochemical cycling of elemental mercury: anthropogenic influences, Geochim. Cosmochim. Acta, 58, 3191–3198, 1994.

Mason, R. P., Morel, F. M. M., and Hemond, H. F.: The role of microorganisms in elemental mercury formation in natural waters, Water Air Soil Pollut., 80, 775–787, 1995.

Mason, R. P., Rolfhus, K. R., and Fitzgerald, W. F.: Mercury in the North Atlantic, Mar. Chem., 61, 37–53, 1998.

Mason, R. P., Lawson, N. M., and Sheu, G. R.: Mercury in the Atlantic Ocean: Factors controlling air-sea exchange of mercury and its distribution in the upper waters, Deep Sea Res. 48, 2829–2853, 2001.

Morel, F. M. M., Kraepiel, A. M. L., and Amyot, M.: The chemical cycle and bioaccumulation of mercury, Annu. Rev. Ecol. Syst., 29, 543–566, 1998.

Narukawa, M., Sakata, M., Marumoto, K., and Asakura, K.: Air–sea exchange of mercury in Tokyo Bay, J. Oceanogr., 62, 249–257, 2006.

Nguyen, H. T., Kim, K. H., Kim, M. Y., Hong, S., Youn, Y. H., Shon, Z. H., and Lee, J. S.: Monitoring of atmospheric mercury at a global atmospheric watch (GAW) site on An-Myun Island, Korea, Water Soil Air Pollut., 185, 149–164, 2007.

Nguyen, H. T., Kim, M. Y., and Kim, K. H.: The influence of long-range transport on atmospheric mercury on Jeju Island, Korea, Sci. Total Environ., 408, 1295–1307, 2010.

Pacyna, E. G., Pacyna, J. M., Sundseth, K., Munthe, J., Kindbom, K., Wilson, S., Steenhuisen, F., and Maxson, P.: Global emission of mercury to the atmosphere from anthropogenic sources in 2005 and projections to 2020, Atmos. Environ., 44, 2487–2499, 2010.

Parker, J. L. and Bloom, N. S.: Preservation and storage techniques for low-level aqueous mercury speciation, Sci. Total Environ., 337, 253–263, 2005.

Poissant, L., Amyot, M., Pilote, M., and Lean, D.: Mercury water–air exchange over the upper St. Lawrence River and Lake Ontario, Environ. Sci. Technol., 34, 3069–3078, 2000.

Poulain, A. J., Amyot, M., Findlay, D., Telor, S., Barkay, T., and Hintelmann, H.: Biological and photochemical production of dissolved gaseous mercury in a boreal lake, Limnol. Oceanogr., 49, 2265–2275, 2004.

Rolfhus, K. R. and Fitzgerald, W. F.: The evasion and spatial/temporal distribution of mercury species in Long Island Sound, CT-NY, Geochim. Cosmochim. Acta, 65, 407–418, 2001.

Rolfhus, K. R. and Fitzgerald, W. F.: Mechanisms and temporal variability of dissolved gaseous mercury production in coastal seawater, Mar. Chem., 90, 125–136, 2004.

Rolfhus, K. R., Lamborg, C. H., Fitzgerald, W. F. and Balcom, P. H.: Evidence for enhanced mercury reactivity in response to estuarine mixing, J. Geophys. Res., 108, 3353, doi:10.1029/2001JC001297, 2003.

Sanemasa, I.: The solubility of elemental mercury vapor in water, Bull. Chem. Soc. Jpn., 48, 1795–1798, 1975.

Schroeder, W. H. and Munthe, J.: Atmospheric mercury – an overview, Atmos. Environ., 32, 809–822, 1998.

Seigneur, C., Karamchandani, P., Lohman, K., Vijayaraghavan, K., and Shia, R. L.: Multiscale modeling of the atmospheric fate and transport of mercury, J. Geophys. Res., 106, 27795, doi:10.1029/2000JD000273, 2001.

Selin, N. E., Jacob, D. J., Park, R. J., Yantosca, R. M., Strode, S., Jaeglé, L., and Jaffe, D.: Chemical cycling and deposition of atmospheric mercury: Global constraints from observations, J. Geophys. Res., 112, D02308, doi:10.1029/2006JD007450, 2007.

Sheu, G. R., Lin, N. H., Wang, J. L., Lee, C. T., Yang, C. F. O., and Wang, S. H.: Temporal distribution and potential sources of atmospheric mercury measured at a high-elevation background station in Taiwan, Atmos. Environ., 44, 2393–2400, 2010.

Shi, J. B., Liang, L. N., Yuan, C. G., He, B., and Jiang, G. B.: Methylmercury and total mercury in sediments collected from the East China Sea, Bull. Environ. Contam. Toxicol., 74, 980–987, 2005.

Sholupov, S., Pogarev, S., Ryzhov, V., Mashyanov, N., and Stroganov, A.: Zeeman atomic absorption spectrometer RA–915+ for direct determination of mercury in air and complex matrix samples, Fuel Process. Technol., 85, 473–485, 2004.

Slemr, F., Brunke, E. G., Ebinghaus, R., Temme, C., Munthe, J., Wangberg, I., Schroeder, W., Steffen, A., and Berg, T.: Worldwide trend of atmospheric mercury since 1977, Geophys. Res. Lett., 30, 1516, doi:10.1029/2003GL016954, 2003.

Slemr, F., Ebinghaus, R., Brenninkmeijer, C. A. M., Hermann, M., Kock, H. H., Martinsson, B. G., Schuck, T., Sprung, D., van Velthoven, P., Zahn, A., and Ziereis, H.: Gaseous mercury distribution in the upper troposphere and lower stratosphere observed onboard the CARIBIC passenger aircraft, Atmos. Chem. Phys., 9, 1957–1969, doi:10.5194/acp-9-1957-2009, 2009.

Soerensen, A. L., Skov, H., Jacob, D. J., Soerensen, B. T., and Johnson, M. S.: Global concentrations of gaseous elemental mercury and reactive gaseous mercury in the marine boundary layer, Environ. Sci. Technol., 44, 7425–7430, 2010a.

Soerensen, A. L., Sunderland, E. M., Holmes, C. D., Jacob, D. J., Yantosca, R. M., Skov, H., Christensen, J. H., Strode, S. A., and Mason, R. P.: An improved global model for air-sea exchange of mercury: high concentrations over the North Atlantic, Environ. Sci. Technol., 44, 8574–8580, 2010b.

Southworth, G. R., Lindberg, S. E., Zhang, H., and Anscombe, F. R.: Fugitive mercury emissions from a chlor-alkali factory: sources and fluxes to the atmosphere, Atmos. Environ., 38, 597–611, 2004.

Sprovieri, F. and Pirrone, N.: Spatial and temporal distribution of atmospheric mercury species over the Adriatic Sea, Environ. Fluid Mech., 8, 117–128, 2008.

Sprovieri, F., Pirrone, N., Gårdfeldt, K., and Sommar, J.: Mercury speciation in the Marine Boundary Layer along a 6000 km cruise path around the Mediterranean Sea, Atmos. Environ., 37, 63–71, 2003.

Sprovieri, F., Hedgecock, I. M., and Pirrone, N.: An investigation of the origins of reactive gaseous mercury in the Mediterranean marine boundary layer, Atmos. Chem. Phys., 10, 3985–3997, doi:10.5194/acp-10-3985-2010, 2010a.

Sprovieri, F., Pirrone, N., Ebinghaus, R., Kock, H., and Dommergue, A.: A review of worldwide atmospheric mercury measurements, Atmos. Chem. Phys., 10, 8245–8265, doi:10.5194/acp-10-8245-2010, 2010b.

Strode, S. A., Jaeglé, L., Selin, N. E., Jacob, D. J., Park, R. J., Yantosca, R. M., Mason, R. P., and Slemr, F.: Air-sea exchange in the global mercury cycle, Global Biogeochem. Cycles, 21, GB1017, doi:10.1029/2006GB002766, 2007.

Strode, S., Jaeglé, L., and Emerson, S: Vertical transport of anthropogenic mercury in the ocean, Global Biogeochem. Cycles, 24, GB4014, doi:10.1029/2009GB003728, 2010.

Sun, S., Wang, F., Li, C., Qin, S., Zhou, M., Ding, L., Pang, S., Duan, D., Wang, G., Yin, B., Yu, R., Jiang, P., Liu, Z., Zhang, G., Fei, X., and Zhou, M.: Emerging challenges: Massive green algae blooms in the Yellow Sea, Nature Prec., hdl:10101/npre.2008.2266.1, 2008.

Temme, C., Slemr, F., Ebinghaus, R., and Einax, J. W.: Distribution of mercury over the Atlantic Ocean in 1996 and 1999–2001, Atmos. Environ., 37, 1889–1897, 2003.

USEPA: Mercury report to Congress, EPA–452/R–97–004, Washington, DC, 1997.

USEPA: Method 1631, Revision E: Mercury in water by oxidation, purge and trap, and cold vapor atomic fluorescence spectrometry, Washington, DC, August, 2002.

Wang, Z., Chen, Z., Duan, N., and Zhang, X.: Gaseous elemental mercury concentration in atmosphere at urban and remote sites in China, J. Environ. Sci., 19, 176–180, 2007.

Wängberg, I., Schmolke, S., Schager, P., Munthe, J., Ebinghaus, R., and Iverfeldt, Å.: Estimates of air-sea exchange of mercury in the Baltic Sea, Atmos. Environ., 35, 5477–5484, 2001.

Wanninkhof, R.: Relationship between wind speed and sea exchange over the ocean, J. Geophys. Res., 97, 7373–7382, 1992.

Whalin, L., Kim, E. H., and Mason, R.: Factors influencing the oxidation, reduction, methylation, and demethylation of mercury species in coastal waters, Mar. Chem., 107, 278–294, 2007.

Witt, M. L. I., Mather, T. A., Baker, A. R., De Hoog, J., and Pyle, D. M.: Atmospheric trace metals over the south-west Indian Ocean: Total gaseous mercury, aerosol trace metal concentrations and lead isotope ratios, Mar. Chem., 121, 2–16, 2010.

Xia, C., Xie, Z., and Sun, L.: Atmospheric mercury in the marine boundary layer along a cruise path from Shanghai, China to Prydz Bay, Antarctica, Atmos. Environ., 44, 1815–1821, 2010.